USGS-OFR-92-528 USGS-OFR-92-528

U.S. DEPARTMENT OF THE INTERIOR

U.S. GEOLOGICAL SURVEY

A geologic overview and one-day field guide of the Taos Plateau volcanic field, Taos County, New Mexico

Ren A. Thompson[1]

Nancy J. McMillan[2]

Open-File Report
92-528

1992

1. USGS, Denver, Colorado.
2. New Mexico State University, Las Cruces, New Mexico.

INTRODUCTION

The Rio Grande rift region of northern New Mexico provides an excellent opportunity to examine the interplay of volcanism, extensional tectonism, and sedimentation within the only active continental rift in North America. This field guide provides researchers and students with an overview of the volcanology, petrology, and geochemistry of the Miocene to Pliestocene volcanic rocks of the Taos Plateau and their relation to rift structure and tectonics.

Structure of the Rift Basins of Northern New Mexico

The Rio Grande rift is a late Cenozoic feature in continental crust of Proterozoic age (1.7-1.4 Ga) which, prior to rifting, experienced deformation during the Uncompaghre (late Paleozoic) and Laramide (late Cretaceous to Eocene) orogenies. Rift basins exhibit the same N-S trend as Laramide compressional structures in the southern Rocky Mountains, and are located near the eastern margin of the region affected by Laramide deformation. The rift is a major physiographic and structural feature of the southern Rocky Mountains extending northward from a poorly defined terminus in northern Chihuahua, Mexico, through New Mexico, and into central Colorado (Tweto, 1979). Normal faulting, regional uplift, high heat flow (Decker and others, 1984), and scattered occurrences of volcanic rocks of late Cenozoic age associated with rifting are present as far north as southern Wyoming (e.g., Leucite Hills).

The Rio Grande rift comprises two segments, the northern segment extending northward from Socorro, New Mexico, into Colorado and the southern segment extending south from Socorro into Mexico (Cordell, 1978). In the regionally broader southern segment, the tectonic style and physiography resemble that of the Basin and Range province: extension is distributed over several wide basins, lithospheric thinning and regional extension have reached an advanced stage, and regional elevations are lower than in the north. In the northern segment, rift basins separate the Colorado Plateau on the west from the High Plains to the east and are confined to a narrow axial zone superimposed on a region of high elevation.

During the early stage of rifting, extension-related faults tended to have northwest trends (Aldrich and others, 1986), whereas later Pliocene to Quaternary extension in the Rio Grande rift has produced normal faulting within the axial zone of the rift with predominantly N-S orientations. The younger phase of rifting which followed a period of relative tectonic and magmatic quiescence in the late Miocene (20-12 Ma), is characterized by a narrowing of rift basins, where early basin-fill sediments of the Santa Fe Group are commonly found on the uplifted blocks adjacent to present rift basins (Golombek, 1983). The post-Miocene rejuvenation of rifting was accompanied by widespread, dominantly basaltic volcanism, active regional uplift, and large differential movements on basin-bounding faults that created deep asymmetric basins. In the area of the northern rift from Albuquerque, New Mexico, to Leadville, Colorado, the rift basins are arrayed in en echelon patterns and are offset along commonly northeast-trending oblique structures (fig. 1).

The intense regional northeast structural grain of Proterozoic basement rocks control northeast-trending Cenozoic structures. For example, both the graben faults of the resurgent dome of the Valles caldera (Jemez volcanic field) and the Embudo fault zone (the southern structural boundary of the San Luis basin) strike to the northeast (fig. 1). The Embudo fault zone in addition to several other northeast-trending faults serve as boundaries, or accommodation zones, that separate differentially tilted, rhomb-shaped structural blocks with longest dimensions that are generally coincident with the axis of the northern rift. Independent tilting and rotating of these blocks as structural units bounded by reactivated zones of weakness, produced the pattern of en echelon offsets and opposing tilts of the basins and uplifts of the northern rift segment.

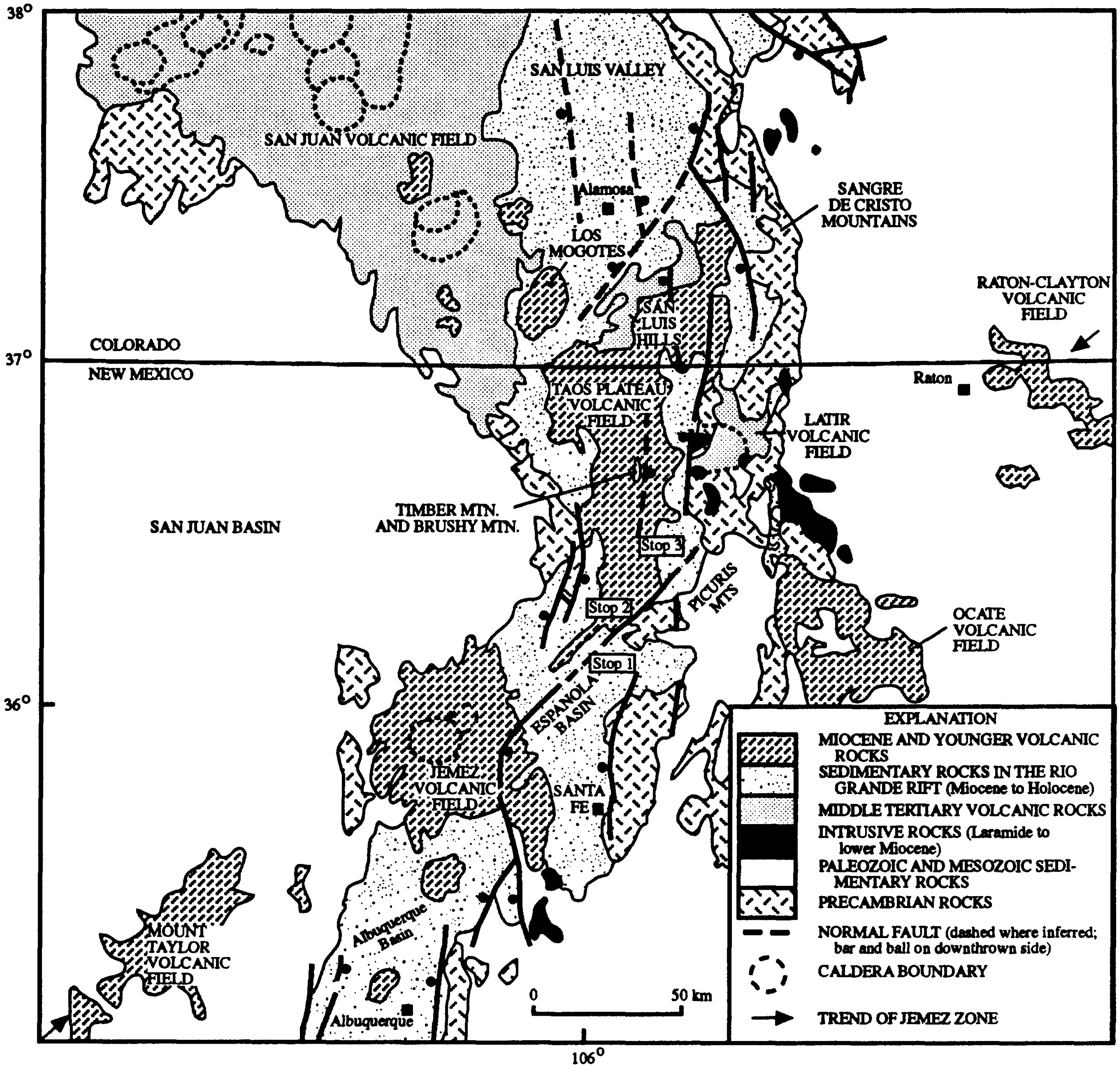

Figure 1.–Generalized geologic map of the Southern Rocky Mountains, showing location of the middle to late Tertiary volcanic fields of the northern Rio Grande rift region and their proximity to major Precambrain uplifts and the Jemez zone. The San Luis basin segment of the Rio Grande rift includes the San Luis Valley and the Taos Plateau underlain by lavas of the Taos Plateau volcanic field.

The San Luis basin is broken into two east-tilted blocks by a northeast-trending fault zone (SE side up) that forms the northern boundary of the structurally high San Luis Hills and creates the reentrant of the front of the Sangre de Cristo Mountains in southern Colorado (fig. 1). Patterns of gravity anomalies of the central San Luis basin show the boundary between these blocks (Keller and others, 1984).

The two San Luis basin sub-blocks have a weak component of southerly tilt as well as a more dominant easterly tilt. This southeasterly dip within the basin opposes the pronounced northerly tilt of the adjacent Sangre de Cristo block (Lipman, 1981), emphasizing the independent motion that characterizes these blocks. On the south of the Embudo fault zone, the Española basin block has apparently undergone counterclockwise rotation (Brown and Golombek, 1985), resulting in compressional structures at the northeastern end of the Embudo zone near Taos and in extension at the southwestern end at Velarde.

The northeast-trending Jemez zone is defined most clearly by an alignment of Miocene and younger volcanic fields (fig. 1) extending from the southeastern margin of the Colorado Plateau (Mt. Taylor volcanic field) through the axis of the rift (Jemez volcanic field) to southeastern Colorado-northeastern New Mexico (Raton-Clayton volcanic field). Thus defined, the Jemez zone crosses several physiographic provinces. The occurrence of these volcanic fields along the Jemez zone has been interpreted as an indication that a major Precambrian crustal shear or suture zone, reactivated by extensional stresses, has acted as a conduit for the mantle-derived magmas that regionally dominate post-Miocene volcanism (Baldridge and others, 1984). However, the striking alignment of the volcanic fields is not matched by evidence that shallow structures within the northeast Jemez zone are important in controlling vent alignments within each volcanic field.

Taos Plateau Volcanic Field

The Taos Plateau volcanic field, in the San Luis basin of northern New Mexico, is one of the largest and most diverse volcanic fields associated with the Rio Grande rift and the Jemez zone, covering approximately 1500 km^2. Compositionally diverse volcanic rocks were erupted over a period of 24 million years (from 26 Ma to 2 Ma) and include tholeiitic basalts, trachybasalts, basaltic trachyandesites, calc-alkaline andesites, dacites, and rhyolites.

Volcanism of three distinct ages is recorded in the Taos Plateau volcanic field (table 1). Early-rift (26-22 Ma) calc-alkaline lavas and pyroclastic rocks associated with the Latir volcanic field are preserved as intra-rift horsts. No volcanic activity has been dated on the Taos Plateau between 20 Ma and 10 Ma, corresponding to a postulated rift-wide mid-Miocene tectonic and magmatic lull (20-12 Ma). However, sporadic basaltic volcanism occurred in the northern Rio Grande rift on the flanks of the Taos Plateau, to the west in the Tusas Mountains, and to the east in the Sangre de Cristo Mountains. A single eruption of quartz latite, Cerro Chiflo, has been dated at 10.2 Ma and represents the only exposed remnant of volcanic activity in the Taos Plateau volcanic field between the early-rift and voluminous Plio-Pleistocene volcanism. Olivine tholeiites, calc-alkaline olivine andesites and two-pyroxene dacites, and rhyolites erupted from 5 Ma to 2 Ma and constitute the predominant volcanic cover of the Taos Plateau.

Oligocene to Miocene volcanic rocks

Dacite, andesite, and rhyolite lavas, and rhyolite ash-flow tuffs exposed on an intrarift horst at Timber Mountain and Brushy Mountain in the San Luis basin (fig. 2) are clearly associated with volcanic rocks of the Latir volcanic field (Thompson and others, 1986). All units exposed on the horst post-date the caldera-forming outflow sheet from the Questa system (fig. 3; the Amalia Tuff) and represent a regeneration of metaluminous magmas similar to the Questa plutons. Lipman (1984) presents a model for the Questa system in which precaldera calc-alkaline magmas, represented by the intrusions, evolve toward more silicic and alkalic compositions, resulting in the mildly alkalic Amalia tuff. Post-caldera magmas return to metaluminous compositions.

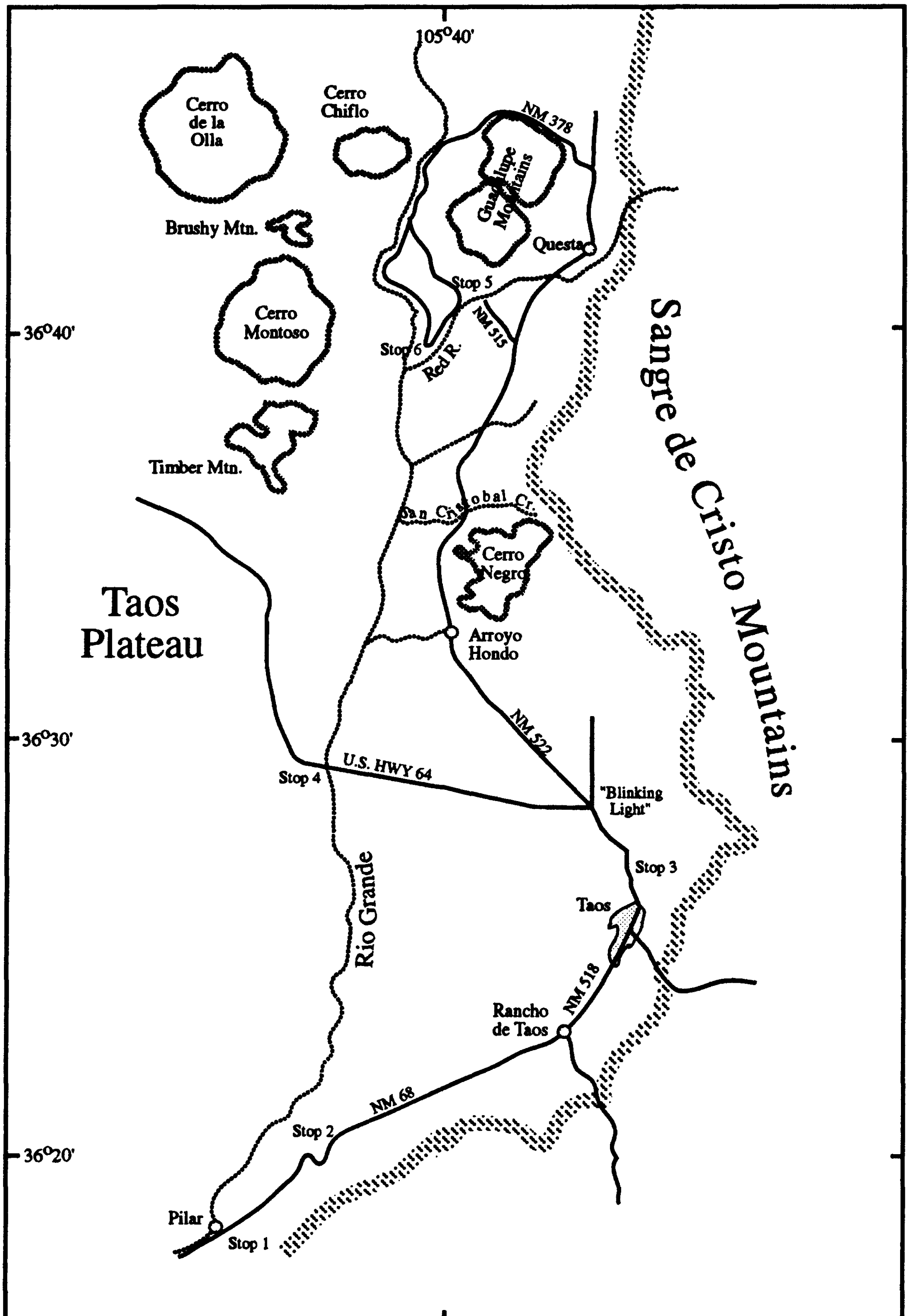

Figure 2.--Generalized location map depicting field guide stop locations and some of the prominant physiographic features discussed in the text.

Two sequences of volcanic rocks are exposed on the horst blocks (Thompson and others, 1986). The lower sequence is dominated by dacite (plag + cpx + opx + Fe-Ti oxides ± hbld), but includes basaltic andesite (ol + cpx + plag) and low-silica rhyolite (plag + san + qtz + bt + Fe-Ti oxides). Dacites contain quenched andesitic micropillows, high-silica rhyolite glass, and sanidine and oligoclase xenocrysts. Incompatible element concentrations increase with silica content throughout the sequence and are accompanied by concomitant decreases in Sr, Sc, and Cr. The upper sequence includes basaltic andesites (ol + cpx + plag), dacite lava flows (plag + hbld + cpx + Fe-Ti oxides + opx + san + sphene ± bt), and a basal lava dome of high-silica rhyolite (qtz + san ± bt ± Fe-Ti oxides ± sphene ± hbld). Upper sequence dacites are distinguished from lower sequence dacites by their hydrous mineralogy and lower relative K_2O, TiO_2, Zr, Y, Nb, Y/Zr, and total REE concentrations at any given silica content.

Major- and trace-element models indicate that suppressed K, Sr, and elevated Mg, Y, and Lu concentrations in the lower sequence dacites resulted from fractionation of phenocryst phases, plus mixing in proportions approaching one to one with high-silica rhyolite similar in composition to the Amalia tuff. Low-silica rhyolites may have been derived through fractionation of dacites plus mixing with the high-silica rhyolite. Positive correlation of $^{87}Sr/^{86}Sr_0$ with SiO_2 are interpreted to reflect the increasing proportions of crustally contaminated high-silica rhyolite in lower sequence, intermediate-composition melts.

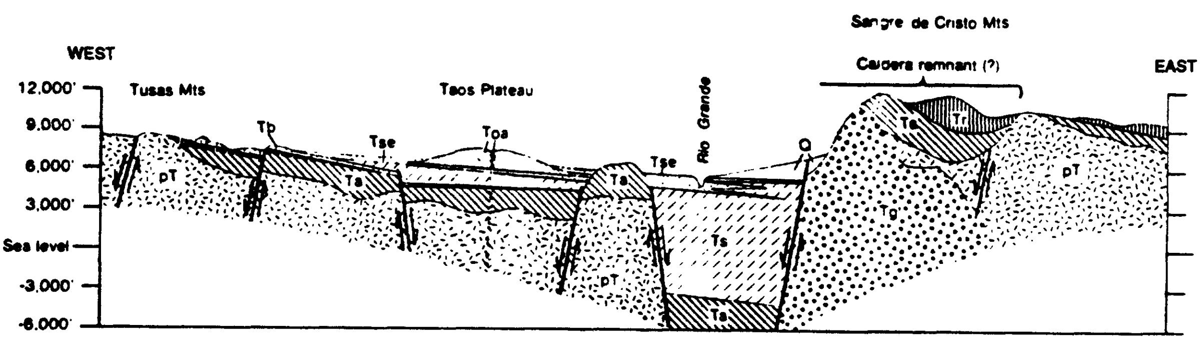

Figure 3.–Cross-section through the Taos Plateau volcanic field, based on general geologic relations at 36°30'N (Lipman and Mehnert, 1979). Symbols: Q, Quaternary surficial deposits; Toa, Plio-Pleistocene olivine andesite; Tse, Plio-Pleistocene Servilleta Basalt; Ts, Tertiary rift sediments; Tb, basalts of the Hinsdale Formation; Tg, granitic intrusions of the Latir volcanic field; Tr, rhyolitic ash-flow tuffs (Amalia Tuff); Ta, post-caldera andesite flows and breccias; pT, pre-Tertiary rocks, mainly Precambrian.

Late-Miocene volcanic rocks

Erosional remnants of two porphyritic quartz latite lava domes are exposed in the Rio Grande gorge at Cerro Chiflo and about 5 km south of Cerro Chiflo. The lava is devitrified, weakly laminated, and contains plagioclase + hornblende ± biotite phenocrysts as well as crustal xenoliths of Precambrian schist, gneiss, and granite (Lipman and Mehnert, 1979). This magma contains about 67 percent SiO_2, and is similar in composition to Plio-Pleistocene two-pyroxene high-silica dacite, in spite of its hydrous mineral assemblage.

Table 1. Volcanism recorded in the Taos Plateau volcanic field

Phase	Location	Lithologies	K-Ar ages
Early-rift (late Oligocene to early Miocene)	Timber Mtn. Brushy Mtn.	Calc-alkaline basaltic andesite, andesite, dacite, rhyolite	26 - 22 Ma
Post-magmatic lull (Miocene)	Cerro Chiflo	Calc-alkaline quartz latite	10 Ma
Late-rift (Pliocene to Pleistocene)	Taos Plateau	Tholeiitic basalt olivine andesite (calc-alkaline); xenocrystic basaltic andesite	5.0 - 3.5 Ma <3.5 Ma

Pliocene to Pleistocene volcanic rocks

Description of lithologies

Plio-Pleistocene volcanic rocks of the Taos Plateau volcanic field are unique among those of the Rio Grande rift volcanic fields because of a scarcity of alkalic basalts and their derivatives, and the dominance of olivine tholeiites (Servilleta Basalt), calc-alkaline olivine andesites and two-pyroxene dacites. Minor lithologies of the Taos Plateau field include trachybasalt to basaltic trachyandesite (formerly called silicic alkalic basalt), xenocrystic basaltic andesite (discussed with the olivine andesites), and rhyolite. Tholeiitic basalts, andesites, and dacites were erupted from monolithologic shield volcanoes (fig. 4) distributed in a semi-concentric pattern (Lipman and Mehnert, 1979). Basalt shields are clustered on the west-central margin of the field, with olivine andesite shields forming a partial ring around them. Two-pyroxene dacite shields, with the exception of a few smaller vents, mark the margins of the field. The larger dacite volcanoes (San Antonio Mtn., Ute Mtn., and the Guadalupe Peaks) are constructed on olivine andesite shields. This distribution may reflect the chemical zoning of the underlying magmatic plumbing system (McMillan and Dungan, 1988) .

Olivine tholeiites of the Servilleta Basalt are by far the major mafic lava composition erupted in the Taos Plateau volcanic field (>200 km^3). These basalts contain olivine ($Fo_{80.5-83}$) + Cr-spinel $\pm$ plagioclase phenocrysts in an ophitic-diktytaxitic groundmass. The development of the diktytaxitic groundmass structure allowed the formation of extensive vesicular segregations as pipes and sheets during post-emplacement in situ crystallization. These segregations are enriched in incompatible trace elements and depleted in Ni and Cr relative to massive portions of the flows (Dungan and others, 1986), and are better developed in flows with coarse diktytaxitic groundmass textures.

Olivine andesites of the Taos Plateau volcanic field (26 km^3) are defined as those calc-alkaline, olivine-bearing volcanic rocks having between 55 and 60 percent SiO_2 (McMillan and Dungan, 1988). The upper SiO_2 content of these andesites is marked mineralogically by the reaction olivine + melt = orthopyroxene. Pyroclastic rocks other than vent spatter are absent and the andesites typically occur as weakly vesicular aa flows on the flanks of monolithologic shield volcanoes. Dacite shields erupted lavas with 60-80 percent SiO_2. Although peripheral dacitic volcanoes developed on top of andesitic shields, the two lithologies are not found intercalated.

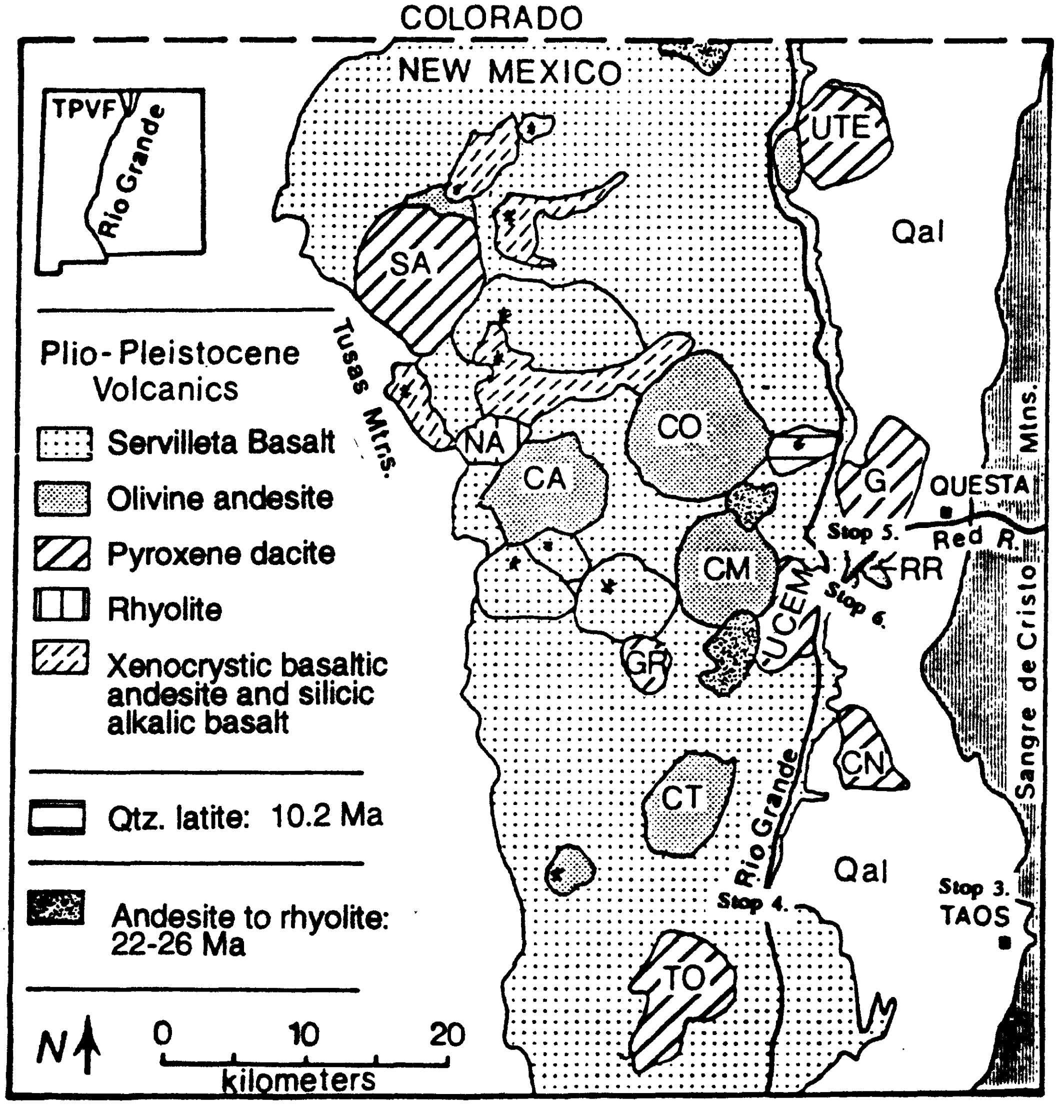

Figure 4.–Distribution of shields, vents and principal lithologies of the Taos Plateau volcanic field. Modified from Lipman and Mehnert, 1979. Volcano names or identifiable locations: SA, San Antonio Mountain; UTE, Ute Mountain; NA, No Agua; CA, Cerro del Aire; CO, Cerro de la Olla; G, Guadalupe Mountain; CM, Cerro Montoso; UCEM, Un-named Cerrito East of Montoso; RR, Red River lavas; GR, Game Ranch dacite; CN, Cerro Negro; CT, Cerro do los Taoses; TO, Tres Orejas. Asterisks indicate shield vent locations.

The andesites contain olivine ± plagioclase ± augite ± orthopyroxene in an intergranular groundmass. Olivine phenocrysts are euhedral to skeletal, weakly zoned, and in equilibrium with whole-rock compositions, indicating that olivine was the liquidus phase of these magmas. The andesites have Mg-numbers equivalent to or slightly lower than the Servilleta basalts, precluding fractional crystallization as the major petrogenetic process. Incompatible trace elements are enriched in the andesites relative to basalt, and have comparable enrichment levels to many of the dacites.

Xenocrystic basaltic andesites (XBA) erupted late in the history of the Taos Plateau volcanic field (K-Ar dates of 2.2 and 1.8 Ma; Lipman and Mehnert, 1979). Compositionally and mineralogically, they are very similar to the olivine andesites, but carry numerous xenocrysts of sodic plagioclase and resorbed quartz.

Taos Plateau two-pyroxene dacites (previously referred to as rhyodacites) form dark-gray to black lava flows that are generally non-vesicular and often contain well-developed internal foliations. They contain augite + orthopyroxene ± plagioclase in a glassy to felty groundmass. Hornblende and apatite are rare phenocryst minerals in the high-silica dacites (SiO_2=65-68 percent). Pyroxene phenocrysts exhibit several zoning patterns and textures (McMillan and Dungan, 1988). Interestingly, orthopyroxene commonly exhibits reverse zoning in orthopyroxene, and rarely in augite. Resorbed Fe-rich cores (En_{70-62}) are surrounded by euhedral Mg-rich rims (En_{82-72}). The boundary is compositionally and optically abrupt. A few orthopyroxene phenocrysts exhibit a core-to-rim Mg-Fe-Mg zoning pattern, again with an abrupt compositional hiatus between zones. These zoning patterns suggest that all of the pyroxenes are magmatic in origin (rather than xenocrystic), and that individual pyroxenes crystallized from magmas that suffered sudden changes in composition.

The tholeiite-andesite-dacite suite forms coherent major element trends from 50 to 68 percent SiO_2 (McMillan and Dungan, 1988). In contrast, incompatible and compatible trace elements do not correlate in a predictable fashion (fig. 5). Although incompatible trace-element concentrations are enriched (up to 17 times) in the dacites relative to Servilleta basalts, many andesites have higher concentrations of these elements than do dacites (fig. 6). In addition, compatible trace elements are enriched in the andesites and dacites relative to levels expected in derivatives of basalt, and in some cases are equal to concentrations in Servilleta basalts. These relationships indicate that the andesites and dacites evolved in an open system, with Servilleta Basalt as the parent.

Trachybasalts and basaltic trachyandesites (SiO_2 = 50-53 percent) are exposed in limited areas in the Taos Plateau volcanic field. These lavas are a minor regional mafic composition, produced fairly late in the evolution of the field, consisting of olivine ± plagioclase phenocrysts in an intergranular groundmass and containing crustal xenoliths.

Four young (3.9 Ma) rhyolite domes are located in the central Taos Plateau volcanic field (No Agua domes, fig. 4). The rhyolite is nearly aphyric, containing less than 1 percent plagioclase + sanidine + quartz (Lipman and Mehnert, 1979). The margins of the domes consist of frothy hydrated perlitic glass with nuggets of obsidian--"apache tears". The interior is devitrified and, in places, flow laminated. The rhyolite has low REE abundances, a large negative europium anomaly, and a high $^{87}Sr/^{86}Sr_o$, indicating a limited interaction between this silicic magma and the majority of the evolving Taos Plateau system.

Volcanic stratigraphy

Stratigraphic relations among Taos Plateau Plio-Pleistocene volcanic rocks are deduced from exposures in the Rio Grande and Red River gorges and from limited areas at the bases of andesitic and dacitic volcanoes. Servilleta basalts were erupted in three major volcanic pulses, producing members named Lower Servilleta Basalt (LSB), Middle Servilleta Basalt (MSB), and Upper Servilleta Basalt (USB; Dungan and others, 1984). These stratigraphic members are separated by clay-rich alluvium derived from the underlying lavas. For the most part, these interbeds lack pebbles and cobbles of Precambrian lithologies exposed in the Sangre de Cristo Mountains. A notable exception is the sediment separating the MSB and USB exposed in the Red River gorge (fig. 7), which represents a prograding alluvial fan deposited by the

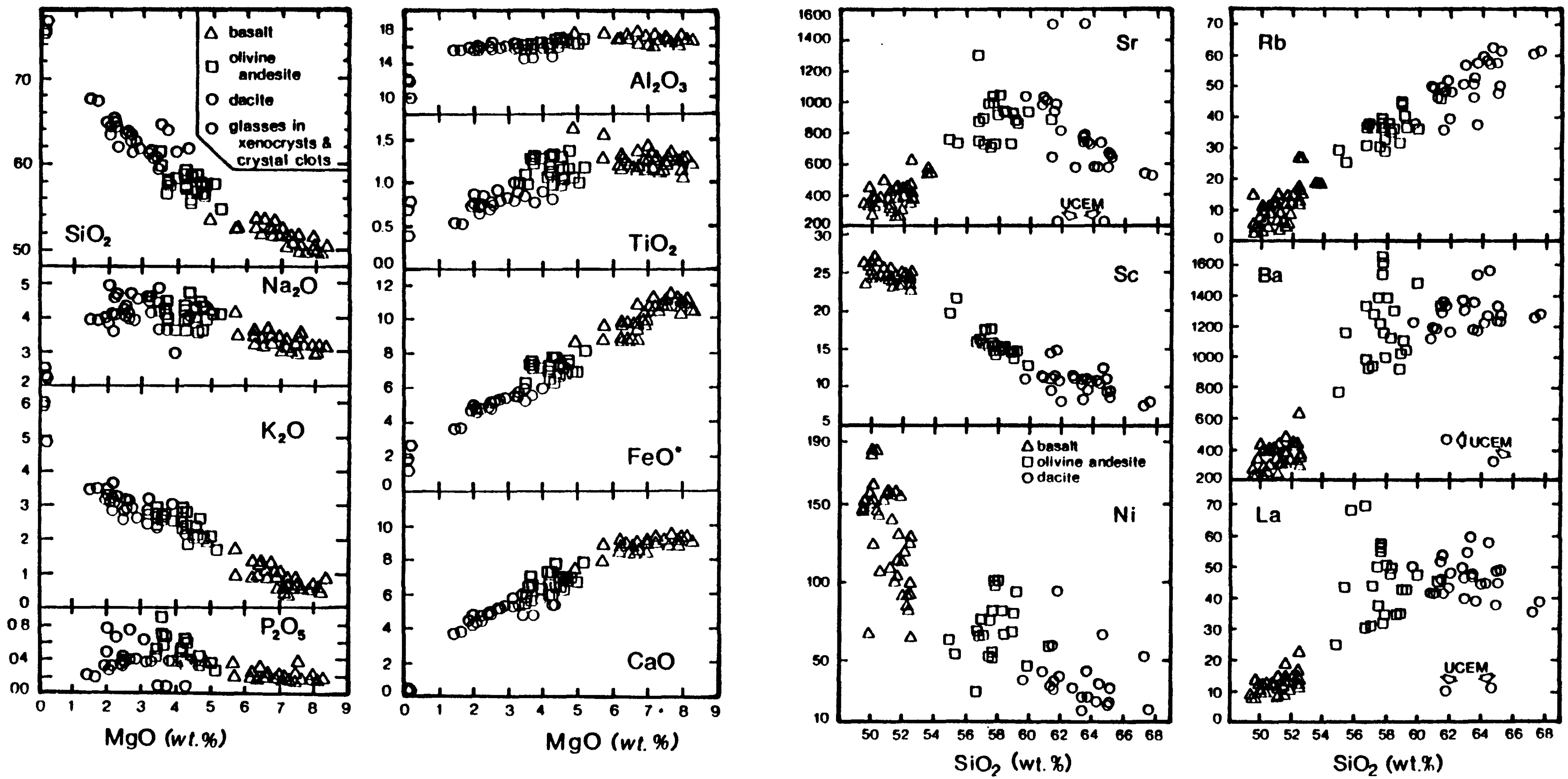

Figure 5.–Major and trace element variation diagrams for the Plio-Pleistocene Taos Plateau basalt-andesite-dacite suite. Major elements in weight percent vs weight percent MgO; trace elements in parts per million vs weight percent SiO_2.

ancestral Red River. The surface of similar alluvial fans formed the topographic base onto which the oldest Taos Plateau volcanic field lavas flowed, and influenced the flow direction of these lavas on the eastern side of the field.

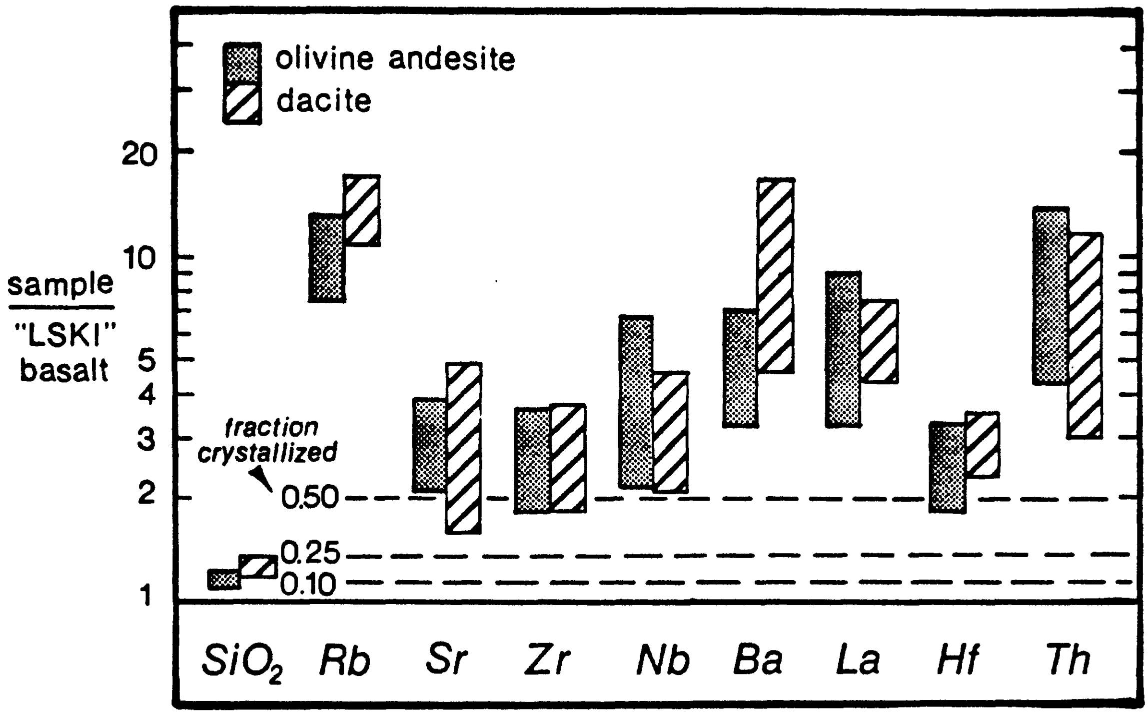

Figure 6.–Elemental enrichment diagram for Taos Plateau olivine andesite and dacites relative to the most primitive LSKI (Low Silica, K_2O, Incompatible trace elements, Dungan and others, 1986) Servilleta tholeiite. Levels of enrichment due to fractional crystallization were calculated using a bulk partition coefficient (D) equal to 0.01 for all elements plotted.

There are two dominant chemical varieties of Servilleta Basalt (Dungan and others, 1984; 1986). The first of these, LSKI basalts (Low Silica, K_2O, Incompatible trace elements; Dungan and others, 1986) are the most primitive compositions erupted in the Taos Plateau volcanic field. Basalts of the second type are found in all three eruptive units and have slightly higher SiO_2 and incompatible element concentrations. LSB and USB contain both types of basalt; MSB is comprised of a third Servilleta variety with higher SiO_2, K_2O, and incompatible element concentrations than the evolved basalts. These lavas, the San Cristobal lavas, have been modeled as mixtures between more typical Servilleta Basalt and magmas similar in composition to olivine andesites or two-pyroxene dacites (Dungan and others, 1986).

The large monolithologic shields of olivine andesite and two-pyroxene dacite mostly post-date or are correlative with the USB. However, stratigraphic relations at several localities in the deeply eroded gorges of the plateau demonstrate there were older periods of intermediate-composition volcanism. Dacite flows are exposed at the base of the section in the Red River gorge (fig. 7). These dacites flowed out onto the alluvial bajada surface (from the Guadalupe vents?) and underlie the LSB. Dacites from the Guadalupe volcanoes separate the MSB and USB in the Rio Grande gorge north of its confluence with the Red River gorge. Another large dacite flow, UCEM

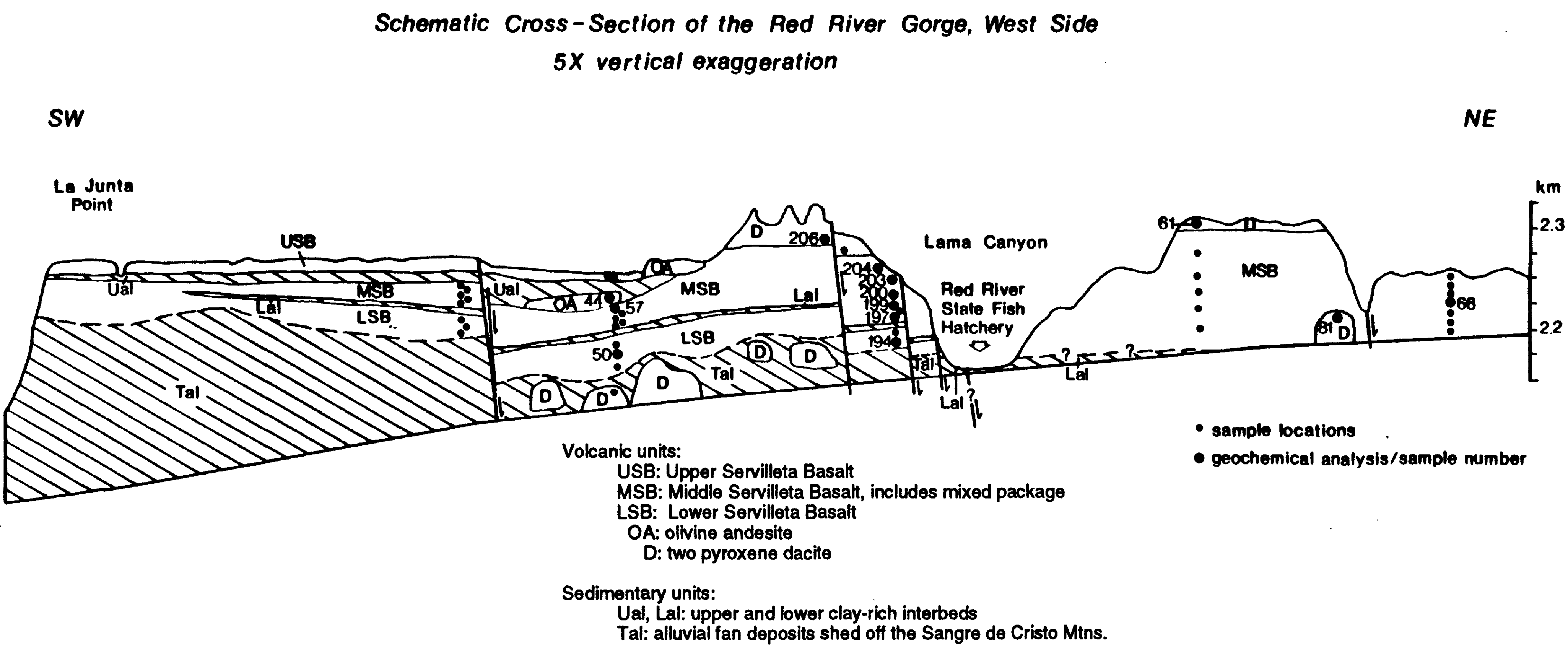

Figure 7.--Schematic cross-section of the Red River gorge drawn from a series of photographs of the western gorge wall. Lava flows of the Red River andesite volcano within unit labled "MSB" extend from the northeast end of the secton approximately to sample number 57.

(Un-named Cerrito East of Montoso), occupies a position between MSB and USB. In the section in the Red River gorge near the Red River State Fish Hatchery, olivine andesites interfinger with MSB flows (fig. 7).

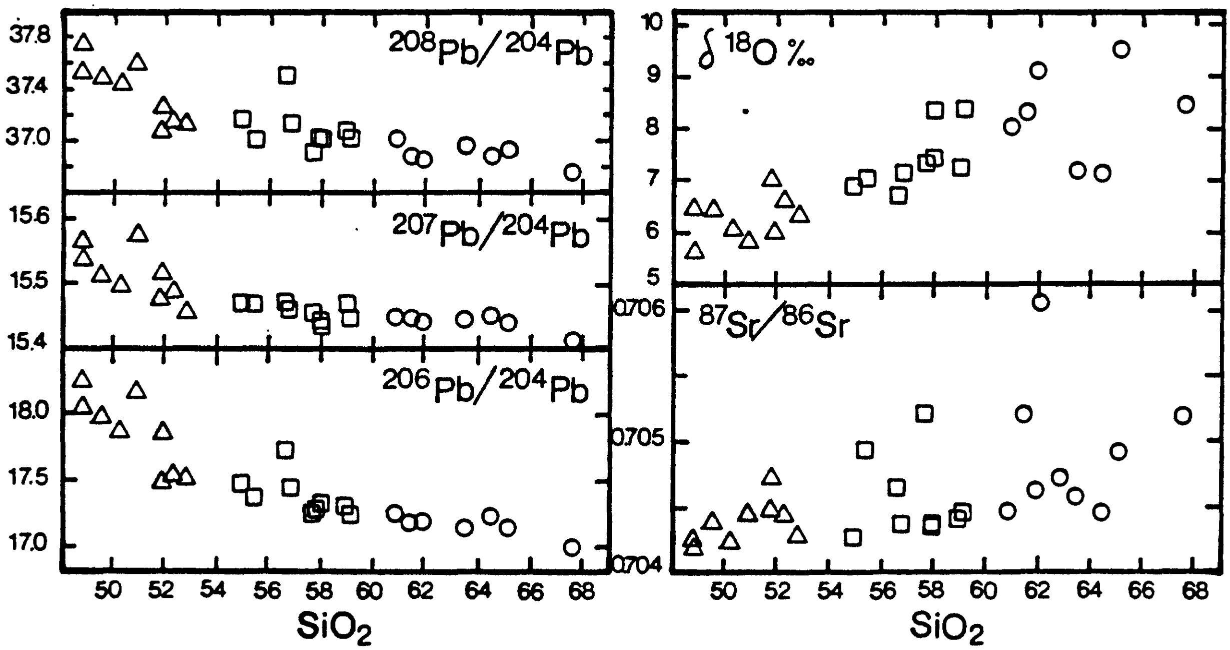

Figure 8.--Radiogenic and stable isotopic ratios for the Plio-Pleistocene Taos Plateau basalt-andesite-dacite suite plotted against SiO_2. Symbols as in figure 5. Whole-rock O-isotope ratios are uncorrected for the effects of secondary H_2O uptake.

The USB exposed in the Rio Grande gorge is locally thinned from San Cristobal Creek (south of Cerro Negro) to the Red River-Guadalupe Mountains area (fig. 4). Young topographic features such as the intrarift horst blocks, UCEM, Cerro Montoso, Cerro de la Olla, and Cerro Chiflo blocked some of the flows from Servilleta vents on the western margin of the field from reaching the eastern portion of the San Luis basin. In addition, the position of the ancestral Red River shifted through time in response to the growth of the andesitic volcano exposed in the northern Red River gorge. Prior to the eruption of the LSB and MSB, the Red River occupied a position similar to its present course and deposited the thick fan that underlies the LSB in the southwestern Red River gorge (fig. 7). Only 8 km to the south, LSB and MSB flows are at or near river level in the Rio Grande gorge where they flowed against the toe of the fan. However, as the Red River volcano grew concomitant with MSB eruptions, it blocked the Red River drainage and deflected sediment transport to the south. As a result, the sedimentary unit separating MSB and USB flows at Garrapata Canyon (5 km south of the Red River) is 75 m thick; in the southwestern Red River gorge, this bed is 15 m thick. The combination of prograding fans and the andesitic shield resulted in a very thin veneer of USB flows along the eastern margin of the field. Eventually, sediment transport to the south was blocked by either prograding fans from the Garrapata and San Cristobal drainages or movement along the Red River fault system, and the Red River established its present position.

Magmatic Evolution

Coherent major-element, trace-element, and isotopic compositions, stratigraphic relationships, and the concentric pattern of vent distribution indicate that the Servilleta olivine tholeiites, olivine andesites, and two-pyroxene dacites are comagmatic. Elevated Mg-numbers and compatible trace-element concentrations in andesites and dacites preclude fractional crystallization of olivine + plagioclase as a dominant differentiation process. The range of compositions have been modeled as having evolved by open-system assimilation, mixing, and fractional crystallization in the lower crust (Dungan and others, 1986; McMillan and Dungan, 1988).

Contamination of Servilleta basalts by depleted lower crust resulted in dacites having lower $^{208}Pb/^{204}Pb$, $^{207}Pb/^{204}Pb$, and $^{206}Pb/^{204}Pb$ than andesites and basalts (fig. 8). The lavas form a linear trend from more radiogenic, mafic compositions to less radiogenic, silicic compositions that is readily explained by contamination with U and Th depleted lower crust. $^{87}Sr/^{86}Sr$ ratios rise slightly as SiO_2 increases, but never exceed 0.70605 (Dungan and others, 1986), again indicating a depleted (low Rb/Sr) contaminant. The UCEM flow exemplifies this type of contamination which has a major element composition similar to other dacites but very low concentrations of most incompatible trace elements (i.e., REE patterns similar to basalt). This occurrence can be modeled as contamination of basalt by partial melts of quartzite, a common Precambrian lithology in northern New Mexico. In addition, the UCEM flows are glassy and contain skeletal olivine and orthopyroxene crystals, that indicate quenching from a superheated state.

Plio-Pleistocene basalts of the Taos Plateau differ from regionally contemporaneous lavas of other Rio Grande rift volcanic fields in Sr- and Nd-isotopic composition because of the influence of depleted lower crust during their petrogenesis (Dungan and others, 1986; Perry and others, 1987). The Taos Plateau basalts plot in an array from near bulk earth to lower $^{143}Nd/^{144}Nd$ and slightly higher $^{87}Sr/^{86}Sr$ values, in contrast to other basaltic suites that lie along the mantle array or have been contaminated by high $^{87}Sr/^{86}Sr$ upper crust. The isotopic composition of many Rio Grande rift basalts can be explained by melting of asthenospheric (ε_{Nd} = +7 to +8) or enriched lithospheric mantle (ε_{Nd} = 0 to +2) as the asthenosphere thermally weakens and erodes the lithospheric mantle (Perry and others, 1988).

Mixing of mafic and evolved magmas to create andesite is indicated by common reversely zoned pyroxene phenocrysts and relatively high Mg-numbers and compatible trace element concentrations in andesites and dacites. This relationship is illustrated by the section exposed at the Red River State Fish Hatchery (fig. 7) in the Red River gorge (McMillan and Dungan, 1986). Here, the MSB is replaced by a section containing basalt (50 percent SiO_2), hybrid basalt (52 percent SiO_2), andesite (55-57 percent SiO_2), and one dacite (61 percent SiO_2). Increasing height of stratigraphic units correlates with increasing SiO_2, K_2O, and incompatible trace element contents, and decreasing MgO, Ni, and Cr contents. Analyses of these lavas define linear trends on all element-element diagrams, forming mixing lines between the compositions of Servilleta Basalt and the dacite that caps the sequence (figs. 9 and 10). Skeletal overgrowths on olivine phenocrysts in the hybrid andesite lavas grew on olivine cores inherited from the basalt end-member during mixing-induced undercooled conditions. The sequence of flows represent eruption of hybrids during mixing; each successive eruption discharged hybrid magmas with an increasing proportion of the dacitic end-member.

The crudely concentric distribution of vents on the Taos Plateau is a reflection of the underlying magmatic plumbing system below (fig. 11). The cluster of Servilleta shields at the west-central margin of the field represents a concentration of magma chambers where the rate of mafic input was large relative to assimilation and crystallization rates. Here, mafic magmas mixed with andesitic or dacitic magmas that had evolved by assimilation and fractional crystallization. The increase in silica content of lavas with distance from the concentration of basaltic vents reflects a decreasing rate of replenishment away from the main mafic conduit system. At the margins of the system, basalt provided heat for assimilation of already warm crust, but mafic input and mixing were subordinate to assimilation and fractional crystallization. Dacitic magmas produced at the margins are the most fractionated compositions in the system. Dacite erupted in the central part of the field indicates that some regions in the central portion of the system were more isolated from mafic input than others. Andesite evolved in an intermediate position, where repetitive mafic recharge supplied the heat required for prolonged assimilation and fractional crystallization, resulting in highly enriched incompatible elements, high Mg-numbers, Cr, and Ni contents.

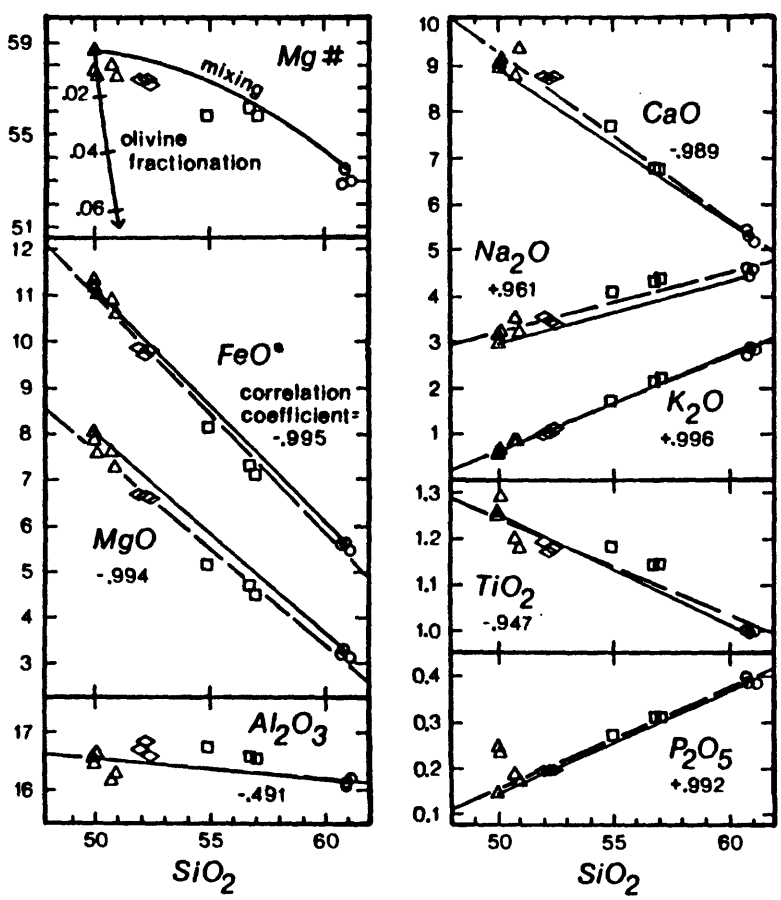

Figure 9.–Major element variation diagram for lavas exposed in the Red River gorge. Oxides as weight percent. FeO* = total iron as FeO, Mg# = 100 x (Mg/(Mg + 0.9Fe)). Symbols as in Figure 5 with the addition of diamonds corresponding to hybrid basalts. Dashed lines represent curves fit by linear regression; solid lines represent simple mixing between basalt and dacite.

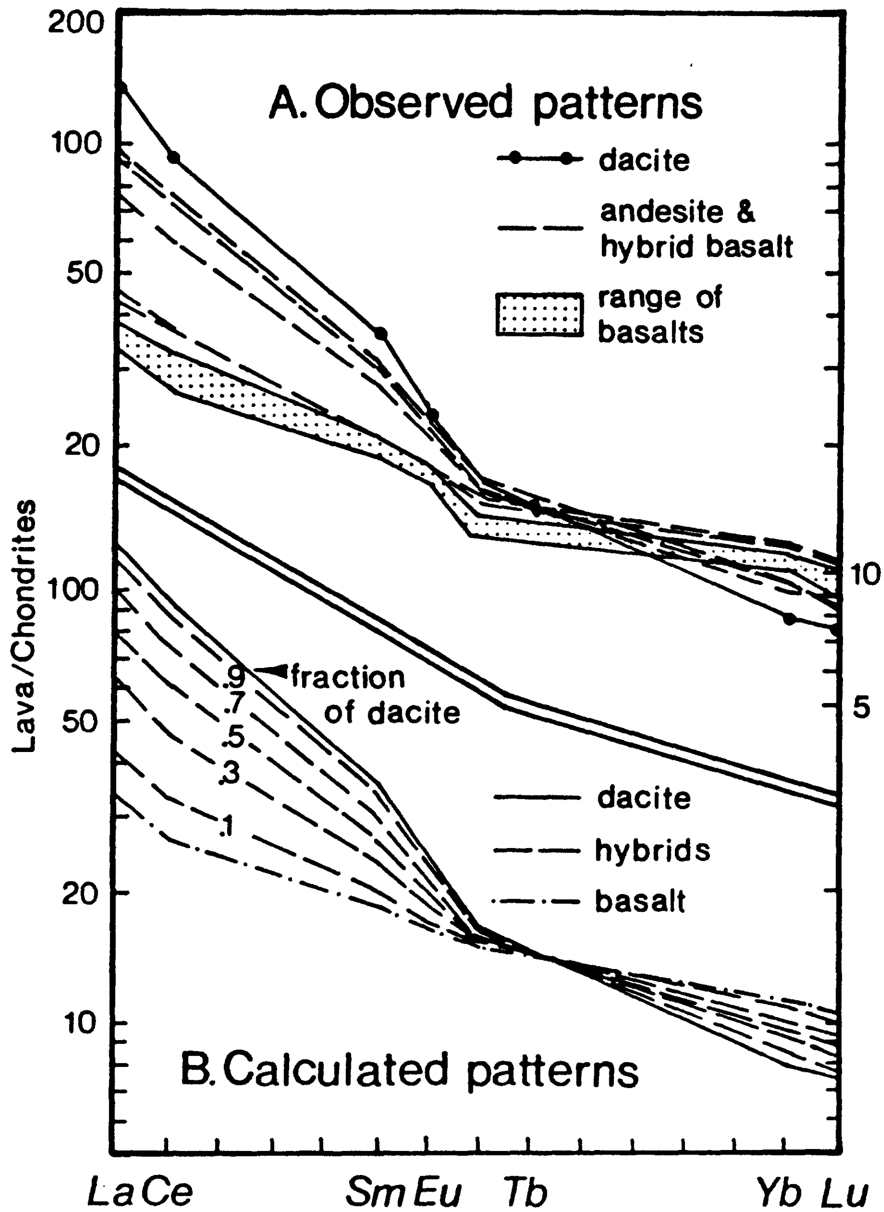

Figure 10.–Composition of observed REE patterns for lavas exposed in the Red River gorge to REE patterns calculated by simple mixing of basalt and dacite.

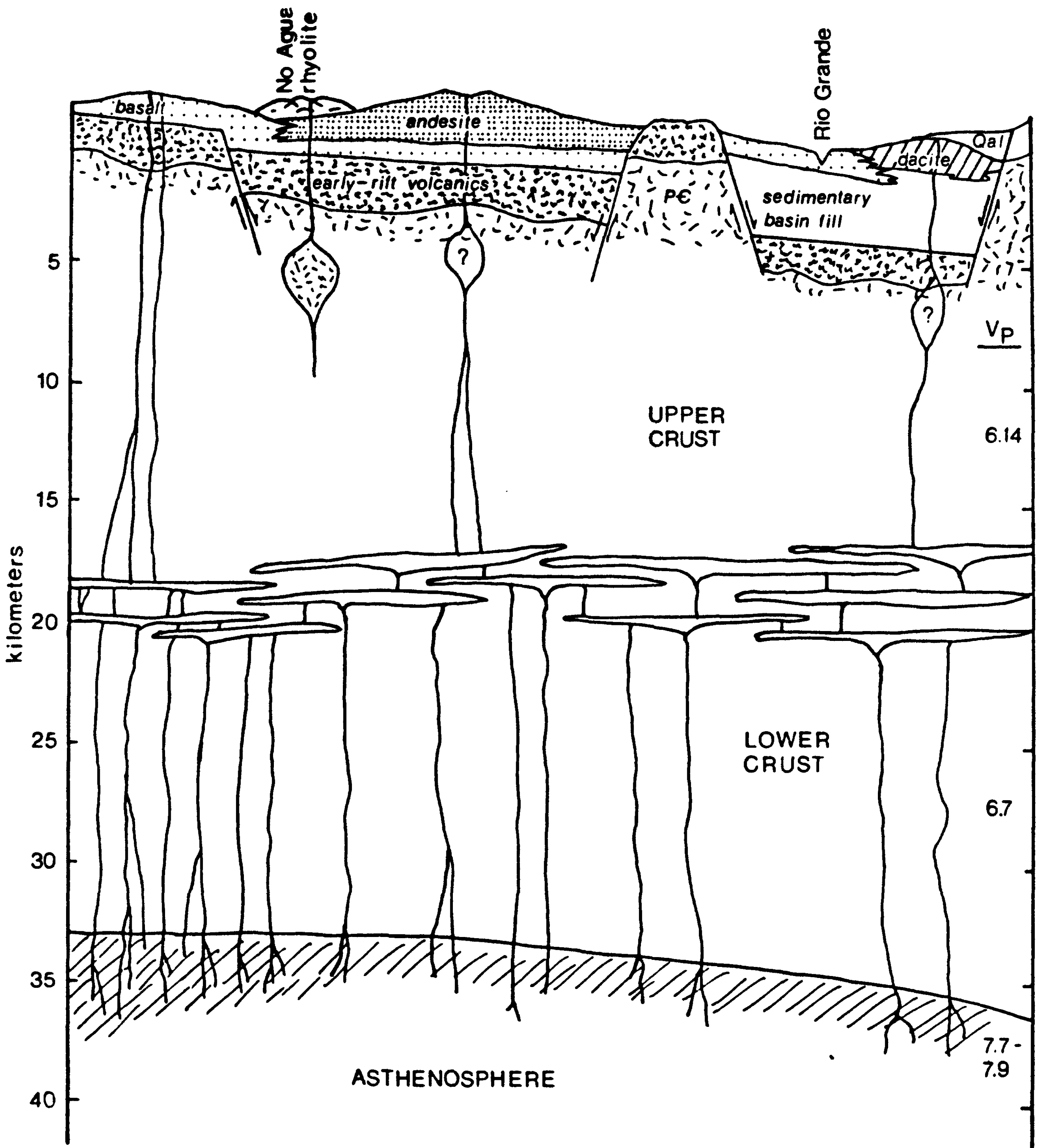

Figure 11.--Cartoon of the Taos Plateau magmatic plumbing system in east-west cross section through the central part of the field. Low mantle Vp values indicate that the asthenosphere is in contact with the lower crust as far north as Albuquerque (Baldridge and others, 1984); there may be enriched lithospheric mantle present in the Taos area. Sill-like interconnected chambers have been drawn at mid-crustal depths analogous to the magma chambers in the Socorro, New Mexico, area. Currently, the only evidence for depth constraints on Taos Plateau magma chambers is that provided by radiogenic isotope studies that indicate mantle-derived basalts were contaminated by old, depleted, lower crustal lithologies (Dungan and others, 1986; McMillan and Dungan, 1986; 1988).

DESCRIPTION OF FIELD TRIP STOPS

This field trip guide presents select Taos Plateau field trip stops from a 1-day field excursion for the 1989 IAVCEI General Assembly. Although this guide is intended to be a stand-alone reference, the reader is encouraged to examine the 3-day field guide to Rio Grande rift volcanism of the northeastern Jemez zone, New Mexico (Dungan and others, 1989) also presented during the IAVCEI General Assembly. The expanded guide includes many additional stops having broader regional interest and scope.

Most of this excursion lies within the eastern half of the USGS Aztec 1:250,000-scale topographic map sheet. The Taos and Wheeler Peak 1:100,000-scale topographic map sheets provide a useful base for following the field-guide route and for locating place names. Unfortunately, subsequent to publication of the 1:100,000 sheets, the New Mexico State Highway Department renumbered some state highways. The new numbers are used in the text.

Road Log

Mileage

0.0 Junction of US-285/84 and NM-68. Drive north through Española, New Mexico, toward Taos on NM-68.

29.2 STOP 1. Embudo fault zone at Pilar, N.M. Cautiously reduce speed, signal a left turn, and turn left into gravel parking area just over the crest of a small hill.

The three axial basins of the northern Rio Grande rift are (south to north) the Albuquerque-Belen, Española, and the San Luis basins (fig. 1). All three are half grabens bounded by major faults on one side and monoclinal flexures on the other. From south to north, the basins exhibit progressive en echelon offsets to the east and reversal in the polarity of tilt; i.e., the Albuquerque-Belen and San Luis basins are tilted to the east and bounded on their eastern margins by high-standing uplifts, whereas the intervening Española basin is tilted to the west. Similar structural geometries have been recognized in other continental rifts such as the East African rift system (Rosendahl, 1987). A complex transcurrent zone of offset, the Embudo fault zone, forms the structural boundary or accommodation zone between the Española and San Luis basins. The Embudo fault zone trends northeast, parallel to the Jemez zone. A component of left lateral strike-slip motion is inferred for the Embudo zone because it forms an oblique continental transform linking the active zone of extension focused on the western and eastern margins of the Española and San Luis basins respectively. The northeast end of the Embudo fault zone is in part compressive, indicating counterclockwise rotation of a rhomb-shaped crustal block that is bounded on the northwest by the Embudo zone (Kelley, 1979; Manley, 1979; Dungan and others, 1984; Brown and Golombek, 1985).

Diktytaxitic olivine tholeiites of the Servilleta Basalt (Lipman and Mehnert, 1975; 1979; Dungan and others, 1986) are the most voluminous lithology (1500 km^2, 200 km^3) of the Taos Plateau volcanic field. Basalt-capped Black Mesa and La Mesita on the southwest represent the southeasternmost extent of the Servilleta Basalt lavas. The distinctive aphyric flows capping these two mesas accumulated in the actively extending Velarde graben and ponded to thicknesses greater than those which characterize the southern Taos Plateau.

Servilleta Basalt capping the southwest part of La Mesita is offset by over 25 meters of normal displacement (down to the northwest) on the Embudo fault.

The trace of one strand of the Embudo fault zone is marked by the excavation scar of an El Paso Natural Gas Co. Pipeline cut into the mesa viewed northward from this stop. Southeast of this fault, a late Pliocene Servilleta Basalt section (two flows) unconformably caps a northwest-dipping Santa Fe sequence consisting of interbedded alluvial-fan and playa sediments. The five Servilleta flows northwest of the fault conformably overlie Santa Fe sediments. The stratigraphic and structural mismatch between Servilleta and Santa Fe sections across the fault indicate significant strike-slip motion along this segment of the fault (Muehlberger, 1979; Dungan and others, 1984).

34.3 **STOP 2. Taos Plateau volcanic field overview.** Park on right in parking lot at top of grade.

Many of the volcanoes of the Taos Plateau volcanic field are visible from this overlook (fig. 4). The plateau surface is formed by the Upper Member of the Servilleta Basalt (USB) and dissected by gorges carved by the Rio Grande and its tributaries. The Rio Grande became entrenched along the eastern margin of the eastward-tilted San Luis basin. As a result, the interplay between alluvial fans prograding westward from the Sangre de Cristo Mountains and basalts flowing eastward from vents on the west-central margin of the field are well exposed in the gorge (Stop 6). Tilting and subsidence of the basin were active concurrent with Servilleta volcanism and continue to the present, as seen by the fan-flow relationships and tilting and arching of the plateau surface. The Rio Grande gorge widens in the southern Taos Plateau area where sedimentary units separating Servilleta Basalt members experience lateral erosion by landslides. The olivine andesitic (OA) and two-pyroxene dacitic (PD) volcanoes visible here are (from left to right): Tres Orejas (PD), San Antonio Mountain (background, PD), Cerro de los Taoses (OA), Cerro Montoso (OA), Cerro Chiflo (ragged skyline, Miocene quartz latite), Ute Mountain (background, PD), and the Guadalupe Mountains (PD). The main cluster of basalt vents form very low-angle shields behind Cerro de los Taoses. The horst blocks are visible in front of Cerro Montoso.

46.0 Intersection of NM-518 and NM-68 in village of Ranchos de Taos. Drive north through Taos. Continue north on NM-518 past the junction of NM-68 and US-64.

52.1 **STOP 3. Recent tectonics in the Taos area.** Park on right shoulder at telephone pole bearing memorial to Tony Gonzales.

Young faults on the Taos Plateau are mostly either north-trending (parallel to the general trend of the San Luis basin and typical of the dominant regional trend of intra-basin structures) or northwest-trending (possibly reactivated faults formed during the early phase of rifting). One such Quaternary fault scarp cuts a large alluvial fan at the foot of Taos Mountain immediately to the east (Dungan and others, 1984; Machette and Personius, 1984; Personius and Machette, 1984). Figure 2 is an idealized cross section of the Taos Plateau at approximately $36^{\circ}30'$N illustrating the asymmetric horst and graben structure of the Taos Plateau region. A major intrarift horst extends most of the length of the Taos Plateau (principally in the subsurface) and exposes remnants of early-rift volcanic rocks associated with the Questa caldera complex that forms the crest of the Sangre de Cristo Mountains to the east. The major basin-bounding normal fault along the Sangre de Cristo range front forms the eastern margin of the Taos Graben, the principal depositional basin on the

Taos Plateau. As much as 1800-2400 meters of sediment fill has been inferred here from geophysical study.

The surface of the plateau is tilted gently to the east-southeast and folded into broad anticlines striking east-northeast. This recent folding has caused drainages cut into unconsolidated alluvium to develop asymmetric profiles with steep channel sides cut farther from the anticline axis. Asymmetrical drainages related to the gorge arch, the best developed of the anticlines, can be seen along US Highway 64 between Taos and STOP 4. After turning west on US Highway 64, note the initial marked asymmetry of the drainages. The size and asymmetry of successive drainages diminishes near the axis of the arch, and then reverses on the west flank.

53.8 Turn left onto US-64 at the "blinking light".

61.9 **STOP 4 High bridge over the Rio Grande and Servilleta Basalt stratigraphy.**

Rejuvenation of the Taos Plateau area has caused entrenchment of the modern Rio Grande, exposing the three members (LSB,MSB,USB) of the Servilleta Basalt. The volcanic section here is nearly 170 m thick, including the sedimentary beds separating the members (total sedimentary thickness is 18 m). Thin sedimentary interbeds separate some flows within the LSB and MSB, indicating periodic hiatus of activity during a major pulse of volcanism. Servilleta basalts are the thickest in this area because flow directions were controlled by thick alluvial fans on the east. Both chemical varieties of Servilleta Basalt, the LSKI and evolved types, are exposed in this section. The LSB is dominantly evolved basalt with one LSKI flow; the MSB and USB here are almost entirely LSKI tholeiites. The characteristic diktytaxitic texture of the Servilleta Basalt can be seen in the uppermost USB flow exposed on the southwest bridge abutment. Servilleta basalts generally contain 5-15 percent olivine phenocrysts, rare plagioclase phenocrysts, and vesicular segregations.

70.0 Return to intersection of US-64 and NM522/NM-518. Turn left (north) onto NM-522.

81.6 Turn left onto NM-515 (New Mexico State Fish Hatchery 2 mi).

83.5 Entrance to Visitor Center. Continue ahead to the left into the southern parking area adjacent to the footbridge across the Red River.

83.65 **STOP 5 Volcanic stratigraphy exposed in the Red River gorge, Red River State Fish Hatchery.**

Tectonic, sedimentary, and geochemical aspects of the evolution of the Taos Plateau volcanic field are represented by exposures of the stratigraphic section in the Red River gorge (fig. 8). In the southwest portion of this gorge (near its confluence with the Rio Grande), the section consists of the LSB, MSB, and USB members of the Servilleta Basalt with no intercalated andesite or dacite. In the northeastern section of the gorge (at the Fish Hatchery and upstream), the MSB interfingers with and is replaced by flows of a small andesitic shield (the Red River volcano). Prior to MSB eruptions, the ancestral Red River likely occupied a position similar to its current location and deposited the thick fan underlying the LSB. The growth of the Red River volcano, however, deflected its flow to the south and formed a small basin between the volcano and the Sangre de Cristo Mountains. As this basin filled, sediment was deposited in a thick alluvial fan to the southwest of the current River (what is now Cebolla Mesa). USB flows originating from vents to the west were unable to flow up onto this topographic barrier, resulting in the thinning of the USB in this area.

Growth faults illustrating contemporaneous sedimentary and tectonic activity are well exposed in the Red River gorge approximately half way between the Fish Hatchery and the Rio Grande confluence (fig. 8). Although sedimentary beds between the MSB and USB on the downthrown block are three to four times thicker than on the upthrown block, MSB and USB units maintain approximate constant thickness across the fault, illustrating that these sedimentary units represent a longer time span than do the volcanic units.

The MSB, andesites from the Red River volcano, and the dacitic flow capping the section immediately downstream from the Fish Hatchery illustrate the importance of magma mixing in the evolution of Taos Plateau intermediate composition lavas (McMillan and Dungan, 1986). Exposed on the northwest wall of the gorge are (from the top down):

1 A single thick dacite flow (RG-206), probably originating from the Guadalupe Mountains to the north

2 A sequence of hybrid basalts (52 percent SiO_2; RG-200, -201, -202) and andesites (55-57 percent SiO_2; RG-302, -2-4), interfingering to the southwest with MSB flows. Lavas in this sequence show increases in SiO_2 and incompatible element abundances with decreases in compatible element abundances and Mg-number with increasing stratigraphic height

3 MSB flows (RG-197, -198, -199)

4 Clay-rich sedimentary interbed lacking Precambrian material from the Sangre de Cristo Mountains

5 LSB flows

6 Clay-rich sedimentary unit with cobbles and pebbles derived from Precambrian rocks in the Sangre de Cristo Mountains

7 Two-pyroxene dacite flows surrounded by alluvial material. These flows are among the oldest evolved Plio-Pleistocene lavas exposed in the Taos Plateau volcanic field.

The sequence of hybrid andesites and dacites display linear trends for all major and trace elements (figs. 9 and 10) between the compositions of Servilleta Basalt and the dacite modeled simply by two-component mixing accompanied by minor (1.5-3.6 percent) olivine fractionation. Hybrid lavas contain olivine and plagioclase phenocrysts in an intergranular groundmass of plagioclase, augite, olivine, and titanomagnetite. Olivine phenocrysts have skeletal hopper morphologies which appear to have grown on euhedral cores inherited from the basaltic end-member during mixing-induced undercooled conditions. Plagioclase phenocrysts exhibit normal-oscillatory zoning and do not record the mixing event. Olivine in the groundmass of the andesites indicates that eruption occurred during or immediately after mixing, because hybrid andesites crystallizing olivine would rapidly exhaust the olivine component in the melt, leaving a plagioclase-pyroxene groundmass.

85.7 Return to intersection of NM-515 and NM-522. Turn left (north) on NM-522.

89.4 Junction of NM-522 and NM-38, continue straight.

92.1 Junction of NM-522 and NM-378. Turn left onto NM-378 toward Cerro, New Mexico, and the Rio Grande Wild River Recreation Area. Continue on paved road to parking area near gorge rim.

100.3 **STOP 6. La Junta Point, confluence of the Rio Grande and Red River.** Turnoff to right leading down to a parking area near the gorge rim. Park and walk to the edge of the gorge.

In the Rio Grande gorge, the UCEM flow lies between the MSB and USB. UCEM is a single, thick, glassy dacite flow containing skeletal orthopyroxene and olivine microphenocrysts. This unusual dacite has high Mg-number and MgO, with low Al_2O_3 and P_2O_5 relative to dacites of comparable SiO_2. Its incompatible trace-element concentrations, with the exceptions of Rb and Th, are identical to Servilleta Basalt (fig. 5). This composition could have been produced by mixing of partial melts of an argillaceous quartzite with basalt (McMillan and Dungan, 1988) .

To the east, erosional remnants of the Questa caldera complex of the Latir volcanic field are seen in the Sangre de Cristo Mountain range front. The Sangre de Cristo Mountains dip to the north exposing Precambrian rocks to the south at the ridgecrest and Cenozoic volcanic rocks of the caldera complex to the north at valley floor levels. Remnants of the Latir volcanic field have been truncated west of the range front by the formation of the Taos graben. Fragmentary exposures of post-caldera volcanic rocks of the Latir field occur directly to the west at Brushy Mountain and 10 km to the south at Timber Mountain. Erosional remnants of the Amalia Tuff, a weakly peralkaline rhyolite are preserved as far as 40 km west of the Questa caldera source.

References

Aldrich, M.J., Jr., Chapin, C.E., and Laughlin, A.W., 1986, Stress history and tectonic development of the Rio Grande rift, New Mexico: Journal of Geophysical Research, v. 91, p. 6199-6211.

Baldridge, W.S., Olsen, K.H., and Callender, J.F., 1984, Rio Grande rift, problems and perspectives, *in* Baldrige, W.A., Dickerson, P.W., Riecker, R.W., and Zidek, J., eds., Rio Grande rift--northern New Mexico: New Mexico Geological Society Guidebook, 35th Field Conference, p. 1-12.

Brown, L.L., and Golombek, M.P., 1985, Tectonic rotations within the Rio Grande rift--Evidence from paleomagnetic studies: Journal of Geophysical Research, v. 90, p. 790-802.

Cordell, Lindrith, 1978, Regional geophysical setting of the Rio Grande rift: Geological Society of America Bulletin, v. 89, p. 1073-1090.

Decker, E.R., Bucher, G.L., Buelow, K.L., and Heasler, H.P., 1984, Preliminary interpretation of heat flow and radioactivity in the Rio Grande rift zone in central and northern Colorado, *in* Baldridge, W.A., Dickerson, P.W., Riecker, R.E., and Zidek, J., eds., Rio Grande rift--northern New Mexico: New Mexico Geological Society Guidebook, 35th Field Conference, p. 45-50.

Dungan, M.A., Lindstrom, M.M., McMillan, N.J., Moorbath, S., Hoefs, J., and Haskin, L.A., 1986, Open system magmatic evolution of the Taos Plateau volcanic field, northern New Mexico: 1--The petrology and geochemistry of the Servilleta Basalt: Journal of Geophysical Research, v. 91, p. 5999-6028.

Dungan, M.A., Muehlberger, W.R., Leininger, L., Peterson, C., McMillan, N.J., Gunn, G., Lindstron, M.M., and Haskin, L., 1984, Volcanic and sedimentary stratigraphy of the Rio Grande gorge and the late Cenozoic evolution of the southern San Luis Valley, *in* Baldridge, W.A., Dickerson, P.W., Riecker, R.E., and Zidek, J., eds., Rio Grande rift--northern New Mexico: New Mexico Geological Society Guidebook, 35th Field Conference, p. 157-170.

Dungan, M.A., Thompson, R.A., and Stormer, J.S., 1989, Rio Grande rift volcanism--northeastern Jemez zone, New Mexico: New Mexico Bureau of Mines and MIneral Resources Memoir, v. 46, p. 435-486.

Golombek, M.P., 1983, Geology, structure, and tectonics of the Pajarito fault zone in the Española basin of the Rio Grande rift, New Mexico: Geological Society of America Bulletin, v. 94, p. 192-205.

Keller, G.R., Cordell, L., Davis, G.H., Peeples, W.J., and White, G., 1984, A geophysical study of the San Luis Basin, *in* Baldridge, W.A., Dickerson, P.W., Riecker, R.E., and Zidek, J., eds., Rio Grande rift--northern New Mexico: New Mexico Geological Society Guidebook, 35th Field Conference, p. 51-57.

Kelley, V.C., 1979, Tectonics, middle Rio Grande rift, New Mexico, *in* Reiker, R.E., ed., Rio Grande rift--Tectonics and magmatism: American Geophysical Union, Washington, D.C., p. 57-70.

Lipman, P.W., 1981, Volcano-tectonic setting of Tertiary ore deposits, Southern Rocky Mountains, *in* Dickinson, W.R., and Payne, W.D., eds., Relations of tectonics to ore deposits in the southern Cordillera: Arizona Geological Society Digest, v. 14, p. 199-213.

Lipman, P.W., 1984, Evolution of the Oligocene-Miocene Questa magmatic system, Rio Grande rift, northern New Mexico, *in* Dungan, M.A., Grove, T.L., and Hildreth, W., eds., Proceedings of the ISEM Field Conference on Open Magmatic Systems, Institute for the Study of Earth and Man: Southern Methodist University, Dallas, Tex., p. 99-101.

Lipman, P.W., and Mehnert, H.H., 1975, Late Cenozoic basaltic volcanism and development of the Rio Grande depression in the southern Rocky Mountains, *in* Curtis, B.F., ed., Cenozoic history of the southern Rocky Mountains: Geological Society of America Memoir 144, p. 119-154.

Lipman, P.W., and Mehnert, H.H., 1979, The Taos Plateau volcanic field, northern Rio Grande rift, *in* Riecker, R.C., ed., Rio Grande rift--Tectonics and magmatism: American Geophysical Union, Washington, D.C., p. 289-311.

Machette, M.N., and Personius, S.F., 1984, Map of Quaternary and Pliocene faults in the eastern part of the Aztec $1^{o}x2^{o}$ quadrangle and the western part of the Raton $1^{o}x2^{o}$ quadrangle, northern New Mexico: U.S. Geological Survey Miscellaneous Field Studies Map MF-1465-B, scale 1:250,000.

Manley, K., 1979, Structure and stratigraphy of the Española basin, Rio Grande rift, New Mexico, *in* Riecker, R.E., ed., Rio Grande rift--Tectonics and magmatism: American Geophysical Union, Washington, D.C., p. 71-86.

McMillan, N.J., and Dungan, M.A., 1986, Magma mixing as a petrogenetic process in the development of the Taos Plateau volcanic field, New Mexico: Journal of Geophysical Research, v. 91, p. 6029-6045.

McMillan, N.J., and Dungan, M.A., 1988, Open system magmatic evolution of the Taos Plateau volcanic field, northern New Mexico: 3--Petrology and geochemistry of andesite and dacite: Journal of Petrology, v. 29, p. 527-557.

Muehlberger, W.R., 1979, The Embudo fault between Pilar and Arroyo Hondo, New Mexico; an active intracontinental transform fault, *in* Ingersoll, R.V., Woodward, L.A., and James, H.L., ed., Santa Fe Country: New Mexico Geological Society Guidebook 30, p. 77-82.

Perry, F.V., Baldridge, W.S., and DePaolo, D.J., 1987, Role of asthenosphere and lithosphere in the genesis of late Cenozoic basaltic rocks from the Rio Grande rift and adjacent regions of the southwestern United States: Journal of Geophysical Research, v. 92, p. 9193-9213.

Perry, F.V., Baldridge, W.S., and DePaolo, D.J., 1988, Chemical and isotopic evidence for lithospheric thinning beneath the Rio Grande rift: Nature, v. 332, p. 432-434.

Personius, S.F., and Machette, M.N., 1984, Quaternary and Pliocene faulting in the Taos Plateau region, northern New Mexico, *in* Baldridge, W.S., Dickerson, P.W., Riecker, R.E., and Zidek, J., eds., Rio Grande rift--northern New Mexico: New Mexico Geological Society Guidebook, 35th Field conference, p. 83-90.
Rosendahl, B.R., 1987, Architecture of continental rifts with special refence to east Africa: Annual Review of Earth and Planetary Sciences, v. 15, p. 445-503.
Thompson, R.A., Dungan, M.A., and Lipman, P.W., 1986, Multiple differentiation processes in early-rift calc-alkaline volcanics, northern Rio Grande rift, New Mexico: Journal of Geophysical Research, v. 91, p. 6046-6058.
Tweto, O., 1979, The Rio Grande rift system in Colorado, *in* Riecker, R.E., ed., Rio Grande rift--Tectonics and magmatism: American Geophysical Union, Washington, D.C., p. 33-56.